Journal of Power Sources 208 (2012) 276–281

Contents lists available at SciVerse ScienceDirect

Journal of Power Sources

journal homepage: www.elsevier.com/locate/jpowsour

Short communication

Preparation and characterization of $La_{0.75}Sr_{0.25}Cr_{0.5}Mn_{0.5}O_{3-\delta}$-yttria stabilized zirconia cathode supported solid oxide electrolysis cells for hydrogen generation

Ruimin Xing[a], Yarong Wang[b], Shanhu Liu[a,*], Chao Jin[c,*]

[a] Institute of Environmental and Analytical Sciences, College of Chemistry and Chemical Engineering, Henan University, Kaifeng 475004, PR China
[b] Department of Laboratory Medicine, Xinxiang Medical University, Xinxiang 453003, PR China
[c] School of Energy, Soochow University, Suzhou 215006, PR China

ARTICLE INFO

Article history:
Received 14 February 2012
Accepted 19 February 2012
Available online 25 February 2012

Keywords:
Solid oxide electrolysis cells
Steam electrolysis
Hydrogen generation
Short-term durability

ABSTRACT

$La_{0.75}Sr_{0.25}Cr_{0.5}Mn_{0.5}O_{3-\delta}$ (LSCM)-YSZ cathode supported solid oxide electrolysis cells (SOECs), with the LSM-YSZ|YSZ|LSCM-YSZ configuration, have been prepared and evaluated for high temperature hydrogen generation. Electrochemical impedance spectra (*EIS*) and voltage–current curves were recorded out to characterize the cell performance. *EIS* results showed that the cell resistance increased as the proportion of steam in the feed supply increased, at open circuit voltage. The hydrogen generation rate calculated from Faraday's law is 561 ml cm^{-2} h^{-1} at 850 °C with 80 vol.% absolute humidity (AH) at a 1.6 V electrolysis voltage. Although there is a 8.2% increase of the applied electrolysis voltage, the cell has endured a test lasting more than 103 h with 45 vol.% AH and 0.33 A cm^{-2} electrolysis current density at 850 °C. Energy-dispersive X-ray (EDX) spectroscopy analysis showed that there is no elemental diffusion between the electrode and electrolyte interface after the durability test. Scanning electron microscopy (SEM) images indicate that the slight split between the LSCM-YSZ cathode and the YSZ electrolyte is responsible for the increase of ohmic resistance of the cell; this resistance rise led to the degradation of the cell performance.

1. Introduction

Hydrogen has been considered as the next generation energy carrier because it is renewable, clean, portable and transportable [1–3]. Compared with reforming methane to generate hydrogen, steam electrolysis using high temperature solid oxide electrolysis cells (SOECs) is a sustainable method for large-scale hydrogen production. It has attracted considerable attention in recent years [4–7].

In principle, SOECs essentially perform the reverse process of solid oxide fuel cells (SOFCs). Consequently, SOEC technology can be built on SOFC technology, which has made significant progress in recent years. In reality, reported studies of SOECs have mainly been based on SOFC research, including studies of electrode and electrolyte materials, cell fabrication methods and stack system designs [8–11]. Ni-YSZ cermet is the usual cathode material for operation of SOECs with a zirconia-based electrolyte. This material displays excellent electro-catalytic properties for steam reduction and enables good current collection at the same time [3,12]. However, the morphology and long-term performance and stability are critical properties of a Ni-YSZ cermet. Under polarization, the predominant micro-structural change in nickel based cermets is the agglomeration and particle coarsening of the metallic Ni [13,14], which leads to a decrease in the length of the three phase boundary (TPB) where the electrochemical reaction takes place. Moreover, the localized surface oxidation of Ni in a high temperature steam environment, to form a less active layer, will also add electrode contact resistance and decrease the SOEC performance. $La_{0.75}Sr_{0.25}Cr_{0.5}Mn_{0.5}O_{3-\delta}$ (LSCM) has a perovskite structure and is a redox stable material with high electrocatalytic properties. It has been reported to be one of the most promising SOFC anode materials for the replacement of Ni-based cermets [15–18]. So far, however, there have been few reports describing the performance of a LSCM cathode based SOEC in a real high temperature steam electrolysis atmosphere. Furthermore, it is well known that thinned electrolytes can decrease the ohmic loss and increase the cell performance but, considering possible chemical compatibility at high temperature, most SOFCs with ceramic materials as electrodes are electrolyte-supported cells [16,17,19,20].

In the present work, a LSCM-YSZ cathode supported SOEC with ~15 μm dense YSZ electrolyte film has been prepared and tested with different concentrations of steam to evaluate its hydrogen generation properties. A durability test of the cell has been performed and a possible degenerative mechanism preventing long-term durability has been detected.

* Corresponding authors. Tel.: +86 13913521956; fax: +86 13913521956.
E-mail addresses: shanhuliu@henu.edu.cn (S. Liu), jinchao@suda.edu.cn (C. Jin).

0378-7753/$ – see front matter © 2012 Elsevier B.V. All rights reserved.
doi:10.1016/j.jpowsour.2012.02.062

2. Experimental

2.1. Preparation and characterization of LSCM material

$La_{0.75}Sr_{0.25}Cr_{0.5}Mn_{0.5}O_3$ (LSCM) was prepared using a citric acid-nitrate process [21]. Stoichiometric amounts of analytical grade lanthanum nitrate ($La(NO_3)_3{\cdot}6H_2O$, Alfa Aesar, 99.9%), strontium nitrate ($Sr(NO_3)_2$, Alfa Aesar, 99.0%), chromium nitrate ($Cr(NO_3)_3{\cdot}9H_2O$, Alfa Aesar, 98.5%) and manganese nitrate ($Mn(NO_3)_2{\cdot}4H_2O$, Alfa Aesar, 98.0%) were dissolved in deionized water with constant stirring at room temperature. The concentration of total metal ions was 0.2 mol L^{-1}. Citric acid was then added to the mixture as a chelating and complexing agent, and the mole ratio of total metal ions: citric acid was controlled at around 1:1.5. Ammonium hydroxide (Sigma–Aldrich, NH_3 content 28.0–30.0%) was added to adjust the pH value to about 6.0. A gel was obtained after the solution was agitated on a hot-plate at 80 °C for 24 h. This was then held in an oven at 400 °C for 5 h to remove organics and form a precursor powder. The $La_{0.75}Sr_{0.25}Cr_{0.5}Mn_{0.5}O_3$ precursor powder was pulverized and then calcined at 1100 °C for 5 h. The crystal structures of the powders were examined by X-ray diffraction (XRD) using a Bede D1 X-ray diffractometer (UK, Bede Scientific Ltd.); Cu K_α radiation; operating at 40 kV, 45 mA; $\lambda = 0.15418$ nm; diffraction angle ranging from 20° to 80° with a step of 0.02° and a rate of 1.2° min^{-1}.

2.2. Fabrication and measurement of the single cell

The as-prepared LSCM and YSZ (TZ-8Y, TOSOH Corporation, Japan) powders were mixed in a weight ratio of 1:1. 20 wt% graphite was added as pore former and the mixture ground in an agate mortar for 8 h. The cathode powders were pressed into pellets 15 mm in diameter and 0.5 mm thick at a pressure of 200 MPa. The green pellets were pre-sintered at 1100 °C for 2 h to obtain the LSCM-YSZ cathode substrates. The dense YSZ electrolyte film was fabricated via a dip-coating method [22]. It was then sintered at 1400 °C for 4 h. The porous anode was prepared using a mixture of $La_{0.8}Sr_{0.2}MnO_{3-\delta}$ (LSM, Fuel Cell Materials, USA) and YSZ in a weight ratio of 1:1 using an ethyl cellulose-terpineol vehicle. The mixture was screen-printed on the YSZ electrolyte film, followed by a pure LSM layer, and fired in air at 1200 °C for 2 h. The effective anode area is 0.33 cm^2. Pt ink was brushed on both LSCM-YSZ cathode and LSM-YSZ anode surface, which was then fired at 1000 °C for 1 h to act as current collector. Pt wires were used to connect the electrodes to the electrochemical testing equipment. The fabricated button cells were sealed to one end of an alumina tube with a ceramic paste (Aremco-552 high temperature ceramic adhesive paste). The ceramic paste was cured during the heating up of the cell electrochemical testing to form a gas-tight seal.

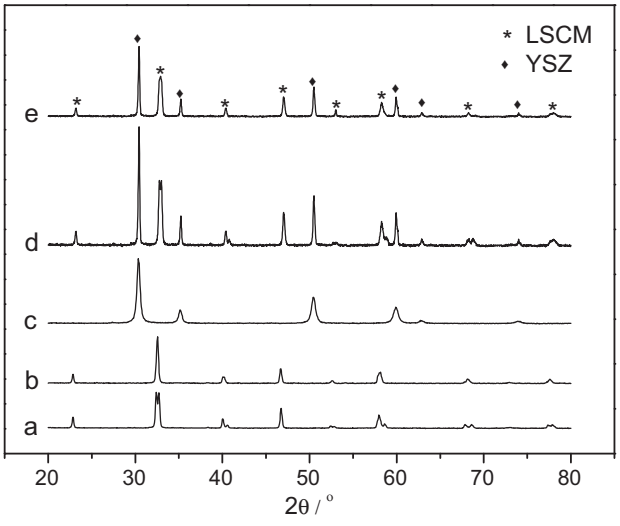

Fig. 1. X-ray diffraction patterns of (a) LSCM powder; (b) LSCM powder reduced by a flow of 30 ml min^{-1} H_2 with 80 vol.% AH at 900 °C for 24 h; (c) YSZ powder; (d) LSCM-YSZ mixture sintered at 1400 °C for 4 h and (e) LSCM-YSZ mixture reduced by a flow of 30 ml min^{-1} H_2 with 80 vol.% AH at 900 °C for 24 h.

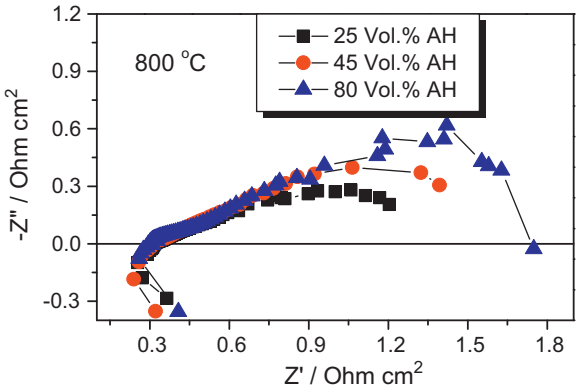

Fig. 2. Impedance spectra of the LSM-YSZ|YSZ|LSCM-YSZ cell measured under OCV with 25, 45 and 80 vol.% AH at 800 °C.

A dedicated high temperature steam electrolysis measurement system and testing procedure have already been clearly described in our previous reports [21,23]. The carrier gas was switched from N_2 to H_2 after the furnace temperature had reached 750 °C in order to maintain the reducing environment in the cathode. The hydrogen flow was controlled at 30 ml min^{-1}. The absolute humidity (AH, the vol.% of humidity. In the total gas volume) was detected using an on-line humidity sensor (Vaisala Model HMP 337) to represent concentration of steam in the electrolysis process. The electrochemical performance of the SOEC cells was studied using a conventional four-electrode method using a multi-channel VersaSTAT (Princeton Applied Research). The electrochemical impedance spectra (*EIS*) under OCV with different concentrations of steam were recorded over the frequency range 100 kHz to 0.1 Hz. The hydrogen generation rate from the SOEC was calculated from Faraday's law, assuming 100% current efficiency [21]. After the durability testing, the cells were cooled down. The microstructure of the cell and the compositions of selected regions of the cell were characterized using a scanning electron microscope (SEM) equipped with energy-dispersive X-ray spectroscopy analysis (EDX) (FEI Quanta 200).

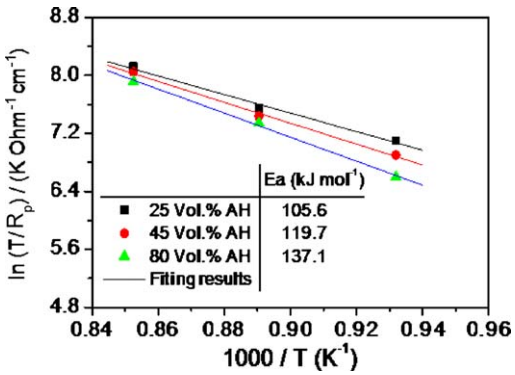

Fig. 3. Arrhenius plots of the electrode polarization resistances for different steam concentrations.

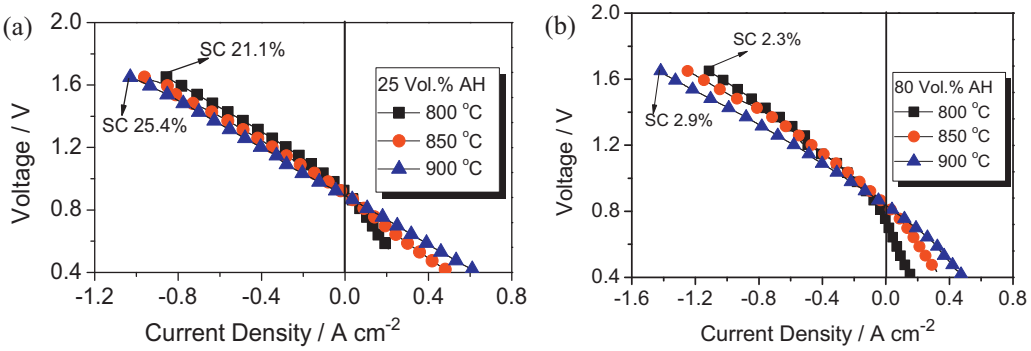

Fig. 4. Voltages–current density curves of the cell with 25 and 80 vol.% AH at different operating temperatures.

3. Results and discussion

3.1. XRD characterization

Fig. 1 shows the XRD patterns of LSCM powders under different conditions. Fig. 1(a) is the XRD pattern of the final LSCM powders after calcination in air at 1100 °C for 5 h, indicating the formation of a single perovskite phase, while Fig. 1(b) is the XRD pattern for the LSCM powders heat-treated by flowing 30 ml min^{-1} H_2 with 80 vol.% AH at 900 °C for 24 h. Compared with the XRD pattern of the pure perovskite phase of the LSCM powders shown in Fig. 1(a), there is no second phase or peak splitting visible in the XRD pattern shown in Fig. 1(b), and the characteristic peaks at 32°, 40°, 58° remain sharp. This result suggests that LSCM is chemically stable in a reducing atmosphere containing a high concentration of steam, which is the typical operating conditions in the cathode of the high temperature electrolysis cells. In the single cell fabrication process, the LSCM-YSZ substrate and green YSZ film have been co-sintered at 1400 °C for 4 h to obtain a dense YSZ electrolyte film. It is therefore necessary to study the chemical compatibility between LSCM and YSZ under high temperature conditions (>1300 °C). Fig. 1(d) displays the XRD pattern of a LSCM-YSZ mixture with a weight ratio of 1:1 sintered at 1400 °C for 4 h. Compared with that of raw LSCM and YSZ powders (shown in Fig. 1(a) and (c), respectively), it can be seen that there is no secondary phase or peak splitting in the XRD pattern of the sintered LSCM-YSZ mixture, suggesting that LSCM is chemically compatible with the YSZ electrolyte at 1400 °C. Furthermore, we also studied the chemical compatibility between LSCM and YSZ in a humidified reducing atmosphere. Fig. 1(e) displays the XRD pattern of a LSCM-YSZ mixture with a weight ratio of 1:1 after heat-treatment in a flow of 30 ml min^{-1} H_2 containing 80 vol.% AH at 900 °C for 24 h. Again, no second phase or peak splitting was detected, and the characteristic peaks of LSCM remained sharp, indicating that LSCM and YSZ are chemically compatible in a humidified reducing atmosphere.

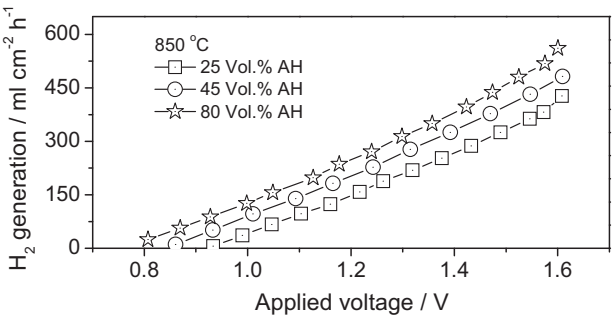

Fig. 5. Theoretical hydrogen generation rate of the prepared single cell with different AH at 850 °C.

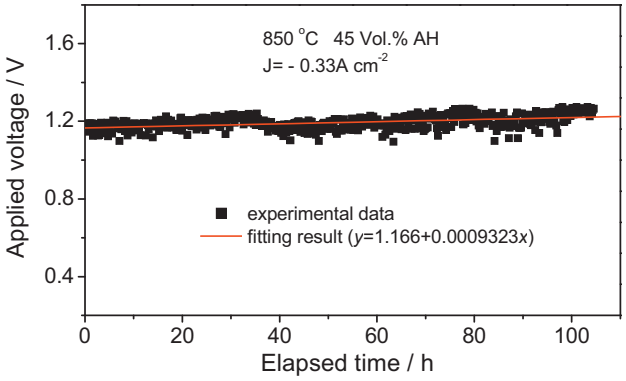

Fig. 6. Short-term durability test with 45 vol.% AH and 0.33 A cm^{-2} electrolysis current at 850 °C.

3.2. Study of electrochemical performance

Fig. 2 displays the electrochemical impedance spectra (*EIS*) of the LSM-YSZ|YSZ|LSCM-YSZ cells measured at open circuit condition with 25, 45 and 80 vol.% AH at 800 °C. The intercept of the impedance spectra with the real axis at high frequency corresponds to the ohmic resistance (R_s) of the cell, which mainly results from the YSZ electrolyte and the Pt lead wires. The overall size of the impedance arcs is attributed to the cell polarization resistance (R_p). The intercept of the impedance spectra with the real axis at low frequency corresponds to the total cell resistance (R_t), including the cell ohmic resistance and polarization resistance. The R_t value with 80 vol.% AH is about 1.8 Ω cm^2, which is similar to that of Ni-YSZ supported SOECs with 50 vol.% AH at 850 °C [24]. It suggests that a LSCM-supported SOEC without additional catalyst can be successfully used in an atmosphere with a high concentration of steam. In addition, the influence of the concentration of steam on the cell performance can be clearly observed in Fig. 3. With the increase of

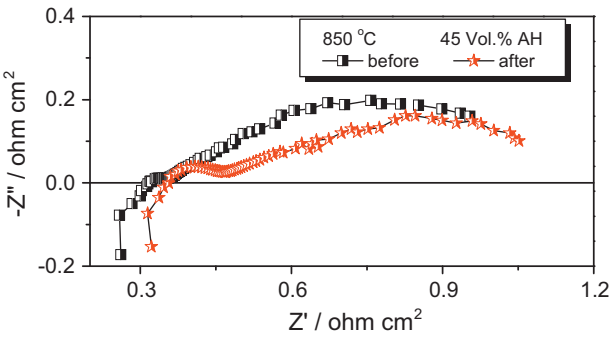

Fig. 7. Impedance spectra of the cell before and after the short-term durability test.

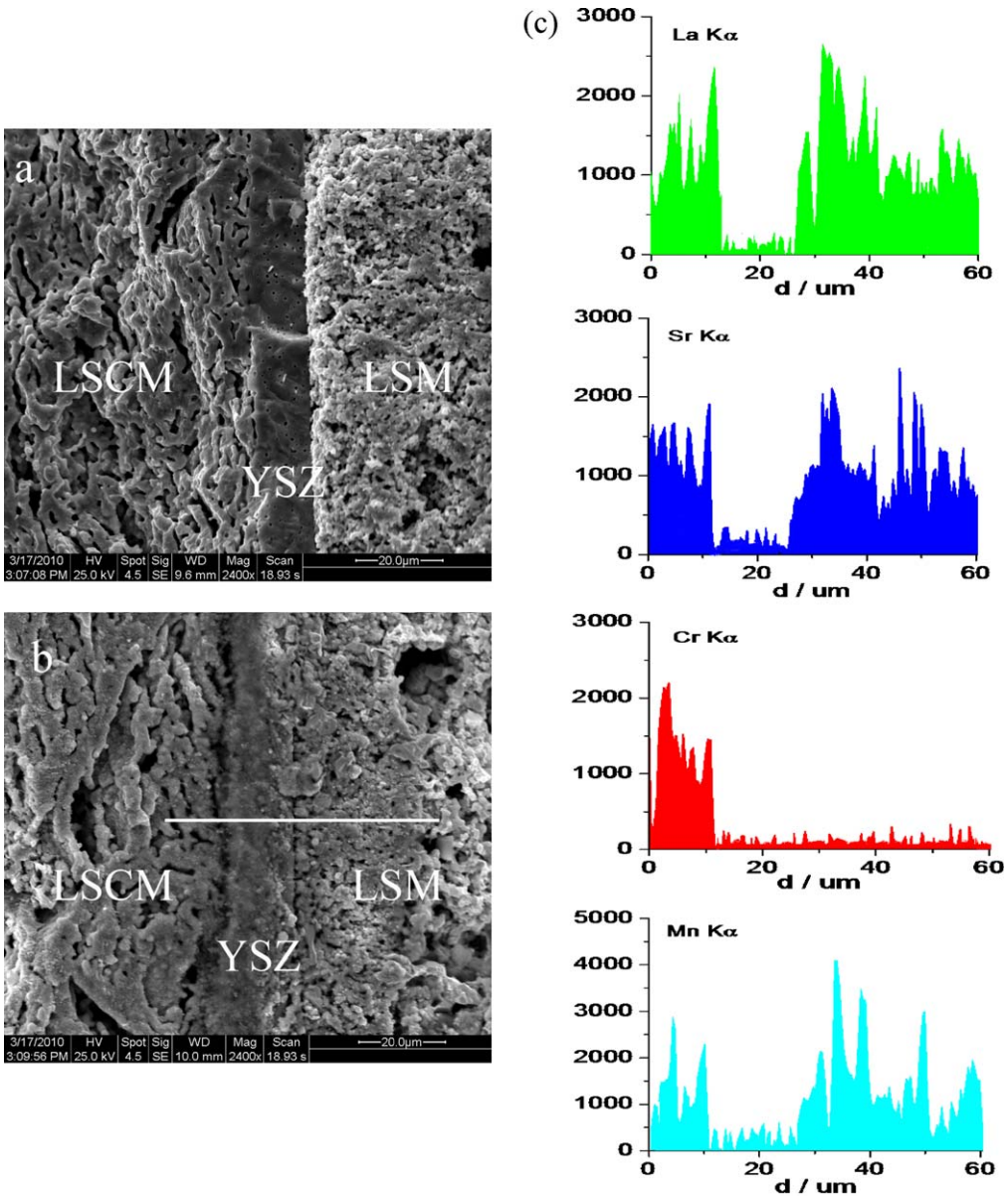

Fig. 8. SEM images of the LSM-YSZ|YSZ|LSCM-YSZ cell (a) before electrochemical test; (b) after short-term durability test and (c) EDX linear scan analysis results of selected region.

steam concentration, R_s is not affected whereas R_p and R_t are considerably increased. This result indicates that the concentration of steam in the feed gas affects the SOEC performance and electrolysis reactions become more difficult as the steam concentration increases.

From to the impedance data obtained at different operating temperatures and open circuit voltage, the temperature dependence of the electrode polarization resistance (R_p) for different steam concentrations can be determined. The results are given in Fig. 3. The apparent activation energy (E_a) can be calculated from the slope of $\ln(T/R_p)$ versus $1000/T$ plots, from the Arrhenius equation. The value of E_a obtained in this study varies from 105.6 kJ mol^{-1} to 137.1 kJ mol^{-1} as the absolute humidity increases from 25 vol.% AH to 80 vol.% AH. This result implies that the electrolysis reaction at the electrode become more difficult with the increase of steam concentration. There are two ways to interpret this phenomenon. One is that there is competitive adsorption of reactant gases (H_2 and steam) on the reactive surfaces adjacent to the reactive three phase boundary (*TPB*); the other is a result of the diffusion of gas transport in porous electrodes [25,26], in which its higher molecular weight limits the gas diffusivity of steam compared with hydrogen.

Fig. 4 shows the typical voltage versus current density dependence (*V–I* curves) for both SOFC and SOEC modes with 25 and 80 vol.% AH steam concentrations at cell operating temperatures of 800, 850 and 900 °C. The data in Fig. 4 were acquired by scanning the potential from 1.6 to 0.4 V with 20 mV s^{-1} increments. Negative values of current density indicate power consumption (the SOEC mode) while positive current densities indicate power generation (the SOFC mode). The cell voltage at zero current density corresponds to the open-circuit voltage (OCV). From the *V–I* curves, it can be seen that there is a smooth transition across the range of open-circuit voltage from SOEC mode to SOFC mode, which indicates that the LSM-YSZ|YSZ|LSCM-YSZ cell is reversible regarding the charge transfer reaction. The consumed current density at a given applied electrolysis voltage generally increases with the increase in the operating temperature. From our previous studies

[23,27], we know that the steam-to-hydrogen conversion (SC) rate can be calculated from Faraday's law. The SC value reflects the level of difficulty of conversion of steam to hydrogen. With a given steam concentration, the SC values show little variation with the increase in the operating temperature. However, with the same operating temperature, the SC values decrease significantly with the increase in steam concentration, from 21.1% with 25 vol.% AH to 2.3% with 80 vol.% AH at 800 °C. These results demonstrate that higher current will be consumed for the same degree of electrolysis if a higher steam concentration is used.

According to the Faraday's law, the amount of hydrogen generated from the SOEC cell is proportional to the volumetric current density supplied during the electrochemical reaction. Assuming 100% current efficiency, this can be expressed as follows [1,2,23]:

$$m = \frac{sMIt}{nF} \quad (1)$$

where m is the mass of the substance, s is the stoichiometric coefficient of the species, M is the atomic or molecular weight, I (A) is the current, t (s) is the elapsed time and n is the number of the electrons involved in the charge transfer reaction. Therefore, the outlet hydrogen volumetric flow rate can be expressed as follows [1,2,23]:

$$N_{H_2,o} = 60 \times 10^3 \times \frac{sMIV_{std}}{nF} \quad (2)$$

where $N_{H_2,o}$ is the outlet hydrogen mass flow rate and V_{std} ($L\,mol^{-1}$) is the volume of 1 mole of gas at standard temperature and pressure. Therefore, the increase of current density values with AH values shows that the hydrogen generation capability of the LSM-YSZ|YSZ|LSCM-YSZ cell increases with the feed steam concentration.

Representative plots of hydrogen generation rate during DC sweeping with 25, 45 and 80 vol.% AH at 850 °C, respectively, are shown in Fig. 5. The hydrogen production rate increases with the increase of the steam concentration, as well as the applied electrolysis voltages. With an applied voltage of 1.6 V and 80 vol.% AH, a theoretical hydrogen generation rate as high as 561 ml cm^{-2} h^{-1} has been achieved, which is much higher than that of a $SrCeO_3$-based ceramic hydrogen permeation membrane at 804 °C (24 ml cm^{-2} h^{-1}) [28,29], indicating that the prepared LSCM-YSZ supported SOEC can be effectively used for high temperature steam electrolysis to produce hydrogen.

3.3. Cell durability study

Although Yang and Irvine investigated the possibility of using LSCM as a cathode material in high temperature steam electrolysis cells, they used a lower steam concentration (3 vol.% H_2O) and the cell durability test was not demonstrated [18]. Fig. 6 shows the short-term durability performance of the cell operated at a constant electrolysis current density of 0.33 A cm^{-2} with 45 vol.% AH and 30 ml min^{-1} H_2 as carrier gas at 850 °C. The cell shows a relatively stable voltage of 1.166 V in the initial operating period of 20 h. After that, the applied electrolysis voltage slowly increased. Compared with the initial applied electrolysis voltage, the voltage increased by 8.2%, from 1.166 to 1.262 V, after operation for more than 103 h. Fig. 7 displays the electrochemical impedance spectra of the cell before and after the durability test. It can be seen that the total cell resistance increased after the durability test, and the change of the ohmic resistance dominated the change of the total resistance, which is the main reason leading to the degeneration of the cell electrolysis performance.

Fig. 8(a) presents a SEM micrograph of the cross-section of the cell before the electrochemical performance test. As shown in Fig. 8(a), the cell has a ~15 μm dense YSZ electrolyte film, and both the LSCM-YSZ cathode and the LSM-YSZ anode adhere very well to the YSZ film. Fig. 8(b) shows the cross-section of the cell after more than 103 h durability test. As indicated by the white line in Fig. 8(b), EDX linear scans for elemental distribution (La, Sr, Cr, Mn) were carried out over the selected region. The results are shown in Fig. 8 (c). No elemental diffusion between electrode and electrolyte interface was detected during the durability testing. In addition, it can be clearly seen that the LSM-YSZ/YSZ/LSCM interface becomes coarse and there is a slight split between the LSCM-YSZ cathode and YSZ electrolyte after the durability testing, as seen by comparing Fig. 8(a) and (b). This phenomenon is the real reason for the increase of the ohmic resistance. During the electrolysis process, LSCM continues to lose lattice oxygen, which leads to a change of the thermal expansion behavior of LSCM, and finally a mechanical split between cathode and electrolyte.

4. Conclusion

LSM-YSZ|YSZ|LSCM-YSZ solid oxide electrolysis cells were prepared and their operation characterized using different steam concentrations (25, 45 and 80 vol.% AH) at 800, 850 and 900 °C. The cell resistance decreases with the increase of operating temperature and increases with an increase in steam concentration at the same operating temperature. At 1.6 V applied voltage and 850 °C operating temperature, the maximum consumed current density increases from 0.96 A cm^{-2} with 25 vol.% AH to 1.25 A cm^{-2} with 80 vol.% AH, and an encouraging theoretical hydrogen generation rate as high as 561 ml cm^{-2} h^{-1} has been achieved with 80 vol.% AH. The cell endured for more than 103 h in the durability testing under electrolysis operation with 0.33 A cm^{-2} and 45 vol.% AH at 850 °C. All the test results indicate that the LSCM-YSZ supported SOEC is feasible for high temperature hydrogen generation.

Acknowledgments

We gratefully acknowledge the financial support of the Natural Science Foundation of China (NSFC, contract no. 21105021 and 21101056). The work was partly supported by the research fund of the Key Laboratory of Fuel Cell Technology of Guangdong Province.

References

[1] J.E. O'Brein, C.M. Stoots, J.S. Herring, P.A. Lessing, J.J. Hartvigsen, S. Elangovan, J. Fuel Cell Sci. Technol. 2 (2005) 156–163.
[2] J.E. O'Brein, C.M. Stoots, J.S. Herring, J.J. Hartvigsen, J. Fuel Cell Sci. Technol. 3 (2006) 213–219.
[3] A. Hauch, S.H. Jensen, S. Ramousse, M. Mogensen, J. Electrochem. Soc. 153 (2006) A1741–A1747.
[4] A. Hauch, S.D. Ebbesen, S.H. Jensen, M. Mogensen, J. Mater. Chem. 18 (2008) 2331–2340.
[5] W. Donitz, R. Schmidberger, Int. J. Hydrogen Energy 7 (1982) 321–330.
[6] S.H. Jensen, P.H. Larsen, M. Mogenson, Int. J. Hydrogen Energy 32 (2007) 3253–3257.
[7] O.A. Marina, L.R. Pederson, M.C. Williams, G.W. Coffey, K.D. Meinhardt, C.D. Nguyen, E.C. Thomsen, J. Electrochem. Soc. 154 (2007) B452–B459.
[8] Z.W. Wang, M. Mori, T. Araki, Int. J. Hydrogen Energy 35 (2010) 4451–4458.
[9] K. Eguchi, T. Hatagishi, H. Arai, Solid State Ionics 86–88 (1996) 1245–1249.
[10] S. Hashimoto, Y. Liu, M. Mori, Y. Funahashi, Y. Fusishiro, Int. J. Hydrogen Energy 34 (2009) 1159–1165.
[11] J.S. Herring, J.E. O'Brien, C.M. Stoots, G.L. Hawkes, J.J. Hartvigsen, M. Shahnam, Int. J. Hydrogen Energy 32 (2007) 440–450.
[12] A. Atkinson, S. Barnett, R.J. Gorte, J.T.S. Irvine, A.J. McEvoy, M. Mogensen, S.C. Singhal, J. Vohs, Nat. Mater. 3 (2004) 17–27.
[13] T. Iwata, J. Electrochem. Soc. 143 (1996) 1521–1525.
[14] J. Sehested, Catal. Today 111 (2006) 103–110.
[15] S. Tao, J.T.S. Irvine, J. Electrochem. Soc. 151 (2004) A252–A259.
[16] S.W. Tao, J.T.S. Irvine, Nat. Mater. 2 (2003) 320–323.
[17] W. Wang, L. Zhang, S.P. Jiang, J. Power Sources 178 (2008) 92–96.
[18] X.D. Yang, J.T.S. Irvine, J. Mater. Chem. 18 (2008) 2349–2354.
[19] Q. Liu, C.H. Yang, X.H. Dong, F.L. Chen, J. Hydrogen Energy 35 (2010) 10039–10044.
[20] G.L. Xiao, C. Jin, Q. Liu, A. Heyden, F.L. Chen, J. Power Sources 201 (2012) 43–48.

[21] C. Jin, C.H. Yang, F. Zhao, D.A. Cui, F.L. Chen, Int. J. Hydrogen Energy 36 (2011) 3340–3346.
[22] C. Jin, J. Liu, L.H. Li, Y.H. Bai, J. Membr. Sci. 341 (2009) 233–237.
[23] C.H. Yang, C. Jin, A. Coffin, F.L. Chen, Int. J. Hydrogen Energy 35 (2010) 5187–5193.
[24] C. Graves, S.D. Ebbesen, M. Mogensen, Solid State Ionics 192 (2011) 398–403.
[25] C. Jin, C.H. Yang, F.L. Chen, J. Electrochem. Soc. 158 (2011) B1217–B1223.
[26] Y. Jiang, A.V. Virkar, J. Electrochem. Soc. 150 (2003) A942–A951.
[27] C.H. Yang, A. Coffin, F.L. Chen, Int. J. Hydrogen Energy 35 (2010) 3221–3226.
[28] W.H. Yuan, L.L. Mao, L. Li, Chin. Chem. Lett. 21 (2010) 369–372.
[29] G.C. Mather, D. Poulidi, A. Thursfield, M.J. Pascual, J.R. Jurado, I.S. Metcalfe, Solid State Ionics 181 (2010) 230–235.